

# A Method for Preserving Battery Life in Wireless Sensor Nodes for LoRa Based IOT Flood Monitoring

Mohd Aizat Mohd Yazid<sup>1</sup>, Ahmad Jazlan<sup>1</sup>, Mohd Zuhaili Mohd Rodzi<sup>2</sup>, Muhammad Afif Husman<sup>1</sup>, and Abdul Rahman Afif<sup>1</sup>

<sup>1</sup>Department of Mechatronics Engineering, Kulliyah of Engineering, International Islamic University Malaysia, 53100 Jalan Gombak, Selangor

<sup>2</sup>School of Computing, Faculty of Engineering, Universiti Teknologi Malaysia, 81310 UTM Johor Bahru, Johor, Malaysia

Email: mdaizat.my@gmail.com, ahmadjazlan@iium.edu.my, mzm28@gmail.com, afifhusman@iium.edu.my, angah.5462@gmail.com

**Abstract**—A common challenge in the implementation of Internet of Things (IOT) Wireless Sensor Networks (WSN) is that the sensor nodes are known to be power hungry devices. The energy stored in the batteries which power up these sensor nodes deplete quickly especially when more data is transmitted to the cloud or when multiple sensors are attached to a single sensor node. In the context of flood and environmental monitoring, increasing the number of sensor nodes in a Wireless Sensor Network is desirable in order to increase the spatial resolution of the data and hence achieve better representation about rising water levels and overall water quality in a particular city. However, having more sensor nodes in a Wireless Sensor Network results in more challenges for the power supply management of the overall Wireless Sensor Network. A drawback of the sensor nodes which are usually powered by Lithium Ion batteries is that there is a limited number of cycles in which a battery can be charged and discharged before the battery is considered to be fully degraded and therefore methods which can lengthen the duration of each charging and discharging cycle will be useful to increase the overall battery longevity. In this paper, a method which combines solar energy harvesting together with a fuzzy logic based algorithm for adaptive sampling is proposed in order to achieve a continuous source of energy for the sensor nodes and also increase the duration between each charging and discharging cycle resulting in batteries which can last for a longer duration. The developed sensor nodes have been deployed to measure river water levels and dissolved oxygen.

**Index Terms**—Flood monitoring, internet of things, LoRa, lithium ion batteries, wireless sensor networks, dissolved oxygen

## I. INTRODUCTION

WSNs consist of multiple sensor nodes that can be densely deployed to gather information from large geographical areas of interest and these sensor nodes are equipped with the ability to transmit data to a cloud, enabling the data to be accessible in any part of the world.

Each sensor node is fitted with at least one or more sensors, a radio transceiver, a microcontroller, and a power supply unit. Although WSNs are an effective means of gathering large amounts of valuable environmental data, the required energy consumption of these sensor nodes to maintain continuous operation is an ongoing challenge [1]–[10]. With the further development of cloud computing, grid computing and Peer-to-Peer networks and deep learning artificial intelligence, the need for WSN has been further expanded to a wider variety of applications. One of the promising applications of WSNs is for environmental and disaster detection systems such as monitoring flood, haze, and landslides. The developers of such WSNs would also need to ensure that there are no accidental false positive triggers in their systems. For flood detection system in particular, the easiest parameter that can be monitored to detect the flooding is the water level in ponds, rivers or drains. Therefore many of the existing flood detection systems have used weatherproof, industry grade ultrasonic sensor to measure rising water levels as an indicator to detect the flood [11]–[14]. The location of the WSN is crucial to collect information about an impending flood. It is preferable to place WSNs in ponds which accumulate water rather than in rivers or drains with flowing water [15]. In addition there needs to be a lead time of at least one hour in order for a flood detection system to be useful.

Other than the measurement of rising water levels with ultrasonic sensors, other water level monitoring methods which have been previously used for detecting impending floods involved measuring the rising water flow rate levels at the coastal areas. When the flow rate is higher than a threshold flow rate, this indicates the likelihood of flooding to occur [16]. In addition to detection of flooding itself, dissolved oxygen measurements can provide some cues about the health hazards posed by the flood such as the degree of contamination of the water in the flooded areas. Therefore, in this study we have dedicated one sensor node for the measurement of rising water levels and a second sensor node to measure Dissolved Oxygen levels in a river.

Currently one of the most successful flood monitoring projects in the world is the Oxford Flood Network which is a collaborative effort between Nominet UK and

---

Manuscript received August 20, 2021; revised March 17, 2022.

This work was supported by the the Malaysian Ministry of Higher Education under the Federal Research Grant Scheme - Grant No: FRGS19-057-0665 and FRGS16-053-0552.

Corresponding author email: ahmadjazlan@iium.edu.my.  
doi:10.12720/jcm.17.4.230-238

ThingsInnovations. The Oxford Flood Network project addresses the limited spatial resolution of the water level data provided by the Environmental Agency in Oxford by enabling more water level sensors to be installed on bridges, culverts and floorboards throughout the city of Oxford through full utilization of LPWAN open source sensor designs and crowdsensing efforts, consequently leading to higher spatial resolution of the data. Overall visualization of rising water levels and flooding throughout Oxford can be achieved in real time.

The Google Flood Forecasting Initiative is another flood monitoring effort which is based on Deep Neural Networks and has proven to have the capability for detecting floods in India and Bangladesh with a longer lead time, enabling earlier evacuations and more coordinated rescue efforts. The primary objective of the forecasting algorithm is to determine whether the water levels in a river are expected to overflow. Hydrologic models were developed such that the input are precipitation and gauge measurements at selected points along the river and the corresponding output will be future values of the river water levels, especially in regions which are prone to flooding.

In this paper, we present a method to lengthen the battery life of the sensor nodes in a Wireless Sensor Network by combining the usage of solar energy harvesting together with adaptive sampling using fuzzy logics. This proposed method reduces the number of charging and discharging cycles of the battery for a particular period, subsequently reducing the battery degradation over time and resulting in longer lasting batteries. A dedicated circuit is designed for each of these sensor nodes which consists of solar energy harvesting, boost converters, an Arduino microcontroller attached to a LoRa communication module, sensors and trickle charge power management ICs. Fuzzy logics is then incorporated into the Arduino code to achieve adaptive sampling to minimize energy usage. Experiments are then conducted to test the battery life while data is being sent to the cloud and visualized using a Losant dashboard. The overall system is then commissioned to measure water levels and dissolved oxygen levels in a pond.

## II. CIRCUIT DESIGN

The circuit which has been designed for the WSN is shown in Appendix 1. Two of these circuits were fabricated. The first circuit was used in the sensor node dedicated for water level measurement and the second circuit was used in the sensor node dedicated for Dissolved Oxygen measurements. The circuit can be divided into four subcomponents, namely the power supply, sensor circuit, communication module and finally the energy harvesting circuit. Three 18650 3800mAh, 3.7 volt Lithium Ion rechargeable batteries are connected in parallel, resulting to a total 11400mAh capacity while maintaining the overall voltage rating to be 3.7 volts. This is to ensure that the sensor node doesn't lose power too soon, while not having too large of a capacity to recharge.

An MT3608 DC-DC step up voltage converter is used to bring up the 3.7 V from the Lithium Ion batteries to a regulated 5V in order to power up the Arduino Nano and all other modules. In theory the MT3608 DC-DC step up voltage converter has the capability to boost voltages as low as 2 volts up to 24 volts. A HC-SR04 ultrasonic sensor was connected the Arduino Nano on the first sensor node while a SEN0237-A dissolved oxygen sensor was connected to the Arduino Nano on the second sensor node.

The circuit allows a solar panel or a mini hydro turbine to be used as a renewable energy source to provide sufficient voltage and current to power up the sensor node. The solar panel has a rating of 6V and 3W. The energy obtained from either the solar panel or mini hydro turbine input will be fed as input into the TP4056 Lithium Ion Battery charging module. The TP4056 Lithium Ion Battery charging module can handle an input voltage range between 4V to 8V which can come from either the solar panel or mini hydro turbine and can provide up to 4.2V and 1A output to charge the Li-ion batteries. This module has a trickle charging feature such that when the battery charge is almost full, the charging will slow down in order to maintain the health of the Lithium Ion batteries. The charging current of the Lithium Ion battery is controlled by the TP4056 Lithium Ion Battery charging module. Lithium batteries are hazardous when overcharged and therefore the TP4056 is useful to prevent overcharging by stopping the charging by bringing down the charging current to 0A when specific voltage conditions have been reached. The INA219 power monitor IC by Texas Instruments is used for measuring the voltage and current of the individual energy sources, which will be used as input for the adaptive sampling algorithm. An NPN 2N2222 bipolar junction transistor being a current controlled device is used as a switch, triggered by the Arduino nano digital pins to either connect or disconnect the energy harvesting circuit to the power circuit hence enabling or disabling the charging of the Lithium Ion batteries. The charging current enters the collector of this NPN transistor. The Arduino Nano digital pin is connected to the base of this NPN transistor. The emitter is connected to the positive terminal of the battery. The INA219 module is used to measure the battery voltage level, which is another input for the adaptive sampling algorithm using fuzzy logic which will be described in further sections. The Arduino Nano uses an ATmega 328P Integrated Circuit by Atmel Corporation. The sensors which are used to measure turbidity, dissolved oxygen and also water levels are interfaced to the ATmega 328P IC which is part of the Arduino Nano board.

### A. Wireless Data Transmission Using LoRa

LoRa which has been developed by Semtech is a Low-Power Wide Area Network (LPWAN) modulation technique using spread spectrum modulation based on chirp spread spectrum technology. In this study we have

used the LoRa RA-02 SX1278 433MHz LoRa communication module as shown in Fig. 1. The module has the advantage of allowing data to be transmitted at a longer range using a lower power consumption as compared to other wireless data transmission such as Zigbee. A star network topology was used, which consists of two sensor nodes and one gateway.



Fig. 1. LoRa communication module

### III. SOFTWARE DEVELOPMENT

Several conditions were implemented on both sensor nodes through the programs uploaded on the Arduino Nano. Charging will only be activated if the battery voltage drops below 3.7 volts. If the battery voltage reaches 4.0 volts the charging will be disabled. The digital pin D3 on the Arduino Nano will send a trigger to the base of the 2N2222 transistor bipolar junction transistor to send a command signal to the INA 219 and enable the charging of the Li Ion battery using energy harvested from a solar panel. The battery voltage is continuously monitored by using an INA 219 which conveys data to the Arduino Nano through SPI communication module addresses namely 0x40, 0x41 and 0x44. All the VCC pins of the INA 219 were connected to a common 5V power supply and the modules were programmed to operate in low power mode when not in use to minimize power usage. All variables are declared as floats. This data is stored locally on the gateway and sent to Losant in a JSON formatted string.

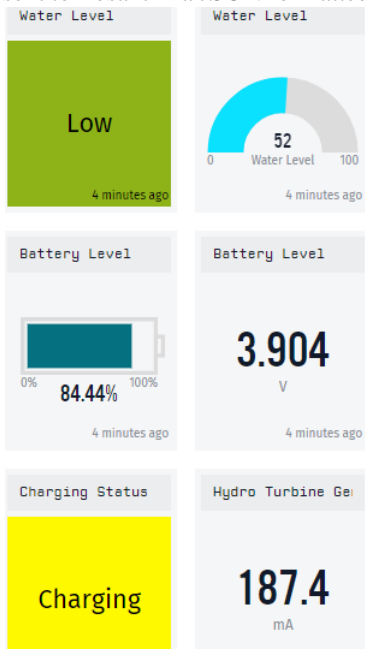


Fig. 2. Losant dashboard

Losant is an IOT cloud service which can be utilized to receive data from wireless sensor nodes. Data can be stored, visualized and analyzed by using the relevant features in Losant. Fig. 2 shows a section of the Losant Dashboard which indicates the real time battery voltage and also water levels sent from the first sensor node.

An algorithm which implements adaptive sampling is developed which makes use of fuzzy logic in order to determine the optimal sampling rate of the sensor in order to lengthen the battery discharging rate. The inputs of this fuzzy logic algorithm are the battery voltage level and the charging current level respectively. The output of this fuzzy logic algorithm is the sampling rate used by the sensor nodes. The sampling rate will be adjusted according to the available voltage levels of the battery and the charging current. Higher voltage levels of the battery and charging current allow a higher sampling rate to be used and subsequently more data being sent to the cloud compared to when the voltage levels and charging current are low since in this case the energy needs to be conserved to keep the sensor node working. The membership functions representing the two inputs and output are presented in Fig. 3, Fig. 4 and Fig. 5 respectively. Table I is a summary of the various conditions of inputs and outputs for this fuzzy logic algorithm.

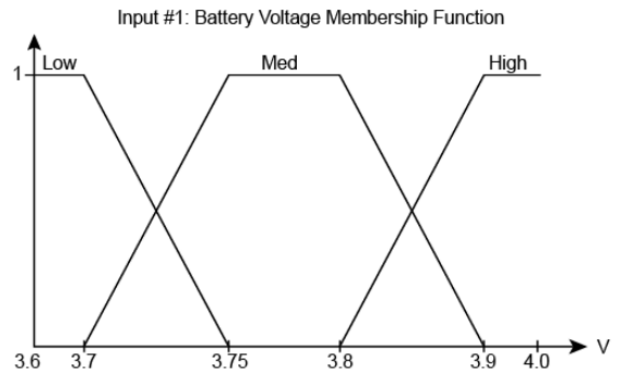


Fig. 3. Membership function for battery voltage

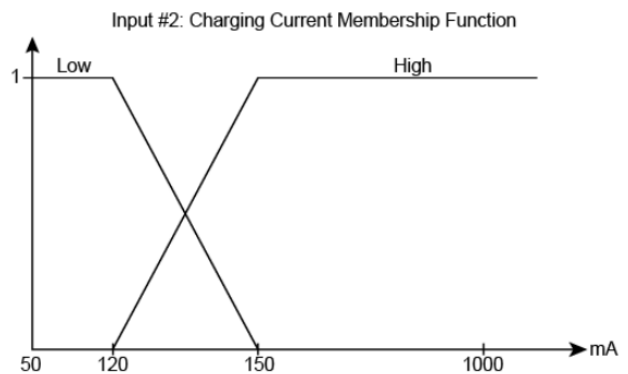


Fig. 4. Membership function for charging current

The Embedded Fuzzy Logic Library (eFLL) has been used to implement this fuzzy logic algorithm on the Arduino Nano. Although Single Board Computers such as NVIDIA Jetson Nano and Rasberri Pi are capable of

performing machine learning methods very efficiently, our primary objective in this study was to minimize power consumption of the sensor nodes and therefore the Arduino Nano was used as the microcontroller for both sensor nodes.

For both the ultrasonic and dissolved oxygen sensors, an internal delay is used such that upon powering up the sensor, data is only collected and transmitted after a 100 millisecond time delay. The sensor node as well as each sensors have its own response time and incorporating a time delay is necessary to accommodate the time lag before the sensor begins to yield accurate readings.

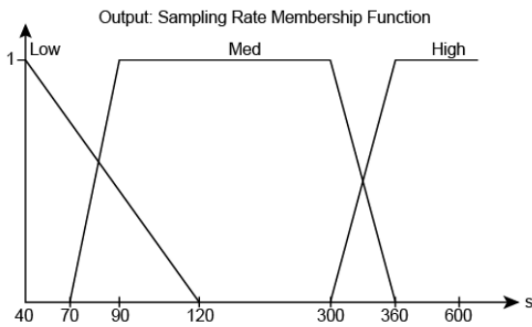


Fig. 5. Membership function for sampling period

TABLE I: FUZZY LOGIC RULES

Battery Voltage	Charging Current	Frequency of Data Transmission
Low	Low	Low
Low	High	Low
Medium	Low	Medium
Medium	High	Medium
High	Low	Medium
High	High	High

#### IV. EXPERIMENTAL RESULTS

Fig. 6 shows the charging and discharging of the set of three 18650 3800mAh, 3.7 volt Lithium Ion rechargeable batteries placed in parallel which was used to power up Sensor Node 1 throughout a 7 day period. During this 7 day period the battery had been fully charged up to 4 volts three times and discharged to 3.7 volts three times as shown in the peaks and trough of the graph in Fig 6. Monitoring the charge and discharge cycle is essential since for Lithium Ion batteries from the very first charge and discharge cycle the capacity of the battery will be subjected degradation over time. Although the battery voltage rating is 3.7 volts it should be noted that this battery can be charged to greater than 4 volts. Throughout this experiment the voltage level of this battery is always kept between 3.7 volts to 4 volts. Fig. 7 shows the battery charging current throughout a 7 day period. Fig. 8 shows the variation of the sampling period or the time interval between two subsequent data transmissions from the sensor node throughout a 7 day period. Sensor node 2 has similar characteristics and therefore the charging characteristics for sensor node 2 is omitted for brevity.

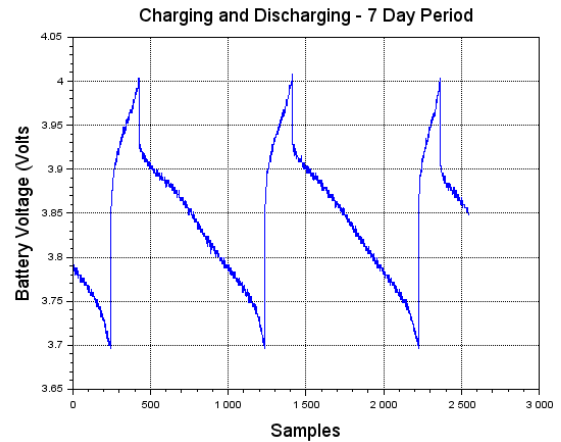


Fig. 6. Charging and discharging of the battery for a 7 day duration

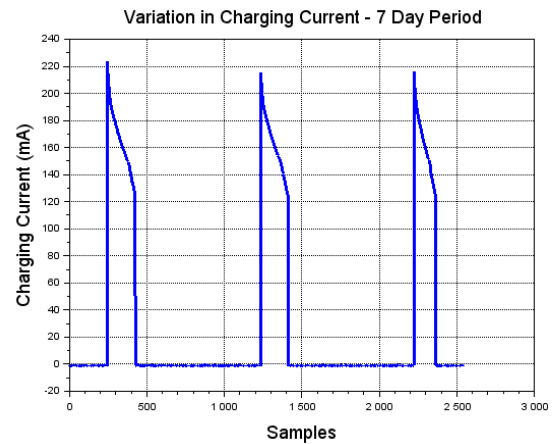


Fig. 7. Charging current for a 7 day duration

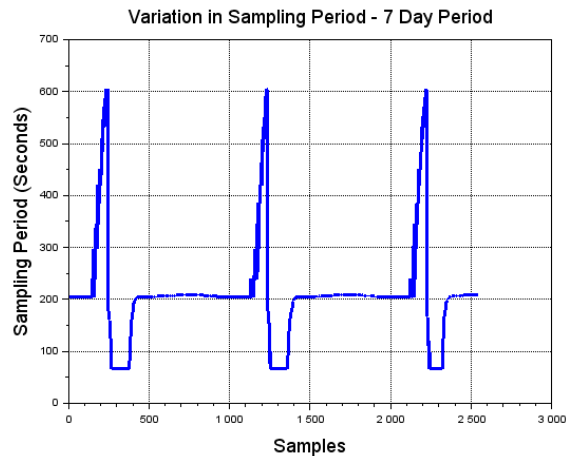


Fig. 8. Sampling Period for a 7 day duration

The initial voltage level for this Lithium Ion parallel battery combination as shown in Fig. 6 was 4 volts and the charging current was zero as shown in Fig. 7 since at this initial starting point charging is deactivated and no battery charging is taking place. The initial sampling period was 200 seconds as shown in Fig. 8. This means that the time interval between two subsequent data transmissions was 200 seconds. During this time interval, the sensor node will be operating in the low power mode to minimize energy consumption. 200 seconds is

categorized as a medium sampling period duration according to the fuzzy logic algorithm which has been developed and this is represented in the membership function shown in Fig. 5. As the Sensor Node 1 was turned on and water level data was being transmitted, the battery voltage gradually dropped down to 3.8 volts as shown in Fig. 6. During this time the sampling period is 600 seconds which means that the time interval between two data transmissions to Losant is 600 seconds. This is the lowest frequency of data transmission since at this point both the battery voltage and charging current are low and therefore the low frequency of data transmission will lengthen the discharging rate of the battery.

As soon as the battery voltage had dropped down to 3.75 volts, charging of the battery begins and the charging current is at its maximum at 220mA as shown in Fig. 7. During this time the sampling period is 60 seconds as shown in Fig. 8 which implies that the highest frequency of data transmission occurs during this period. The combination of a high battery voltage and a high charging current enables having this high frequency of data transmission. The battery will still continue to be discharged to 3.7 volts even though the charging process has started. The battery charging continues until the battery becomes fully charged at 4 volts as shown in Fig. 6. During the battery charging from 3.7 volts to 4 volts, the charging current had dropped from 220mA to 120 mA and finally down to 0mA as shown in Fig. 7 which indicates that charging has been halted when the battery voltage has reached 4 volts. This cycle then continues. The interdependence between the battery voltage, charging current and sampling rate during a 7 day period is shown in the multi axis plot in Fig. 9 which shows a combination of the information presented in Fig. 6, Fig. 7 and Fig. 8 in a single graph.

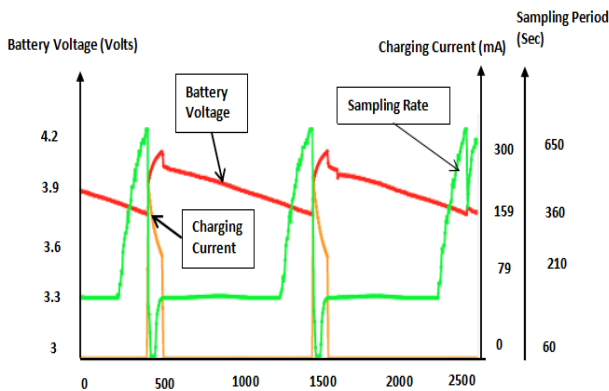


Fig. 9. Multiple axis plot showing interdependence between battery voltage, charging current and sampling period during a 7 day duration

During the overall 30 day period the battery had been fully charged 10 times as shown in the peaks and trough of the graph in Fig. 10. The variation of the charging current and also sampling rate of the data transmission for a duration of 30 days are shown in Fig. 11 and Fig. 12 respectively. The interdependence between battery voltage, charging current and sampling rate during the 30 day period is shown in the multi axis plot in Fig. 13

which shows a combination of the information presented in Fig. 10, Fig. 11 and Fig. 12 in a single graph

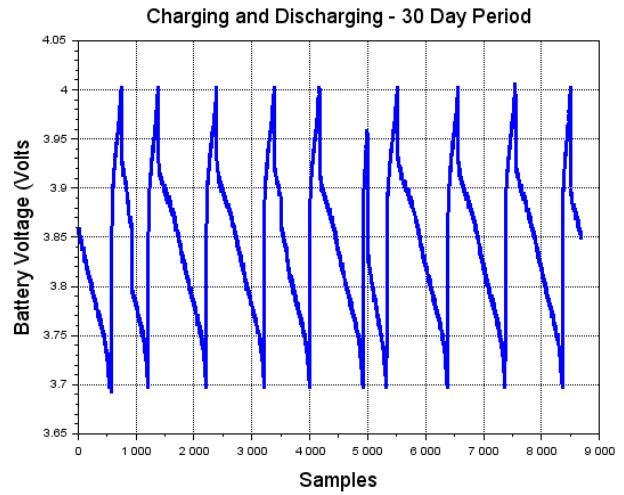


Fig. 10. Charging and discharging of the battery for a 30 day duration

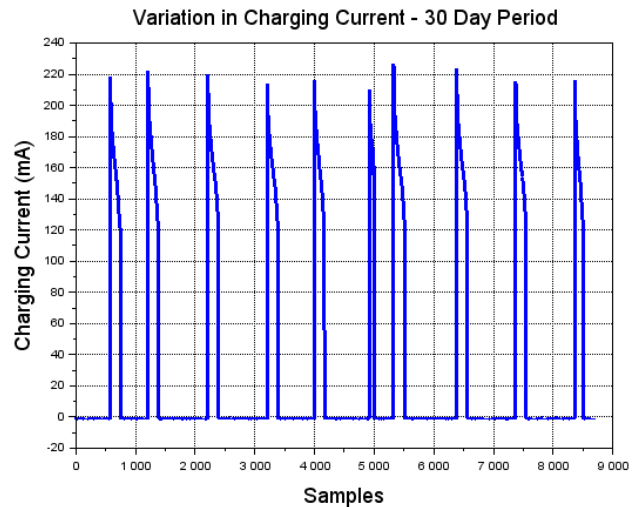


Fig. 11. Charging current for a 30 day duration

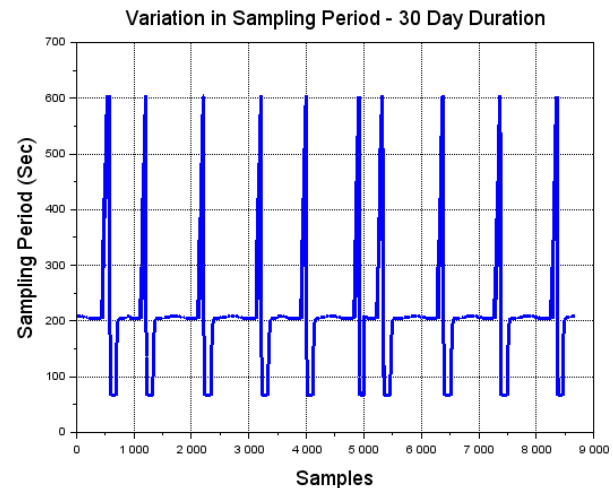


Fig. 12. Sampling period for a 30 day duration

Table II shows a comparison between the number of charging and discharging cycles between the proposed fuzzy logic based adaptive sampling method with the

standard method of data transmission to the cloud with a fixed sampling period in which the data is transmitted to the cloud every 60 seconds. In this experiment it had been proven that although by using the proposed method fewer samples of data were transmitted to the cloud, the results of hydrological parameter monitoring was still reliable as will be described in the following section. By using the proposed method the number of charging and discharging cycles has been reduced and at the same time the sensor nodes are utilizing the availability of solar energy in the Malaysian climate.

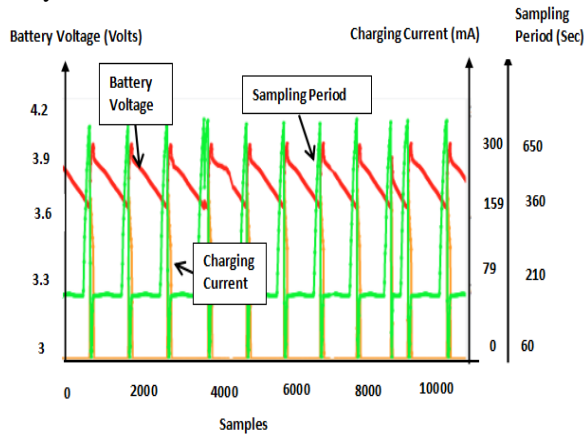


Fig. 13. Multiple axis plot showing interdependence between battery voltage, charging current and sampling period during a 30 day duration

TABLE II: COMPARISON BETWEEN NO. OF CHARGING AND DISCHARGING CYCLES BETWEEN PROPOSED METHOD AND THE FIXED SAMPLING RATE METHOD

No. of Days	No. of Charging and Discharging Cycles (Proposed Method)	No. of Charging and Discharging Cycles (Fixed Sampling Rate)
7	3	6
10	4	8
20	8	16
30	10	25

### V. LORA NETWORK RANGE

Prior to commissioning, the LoRa network has been tested within the International Islamic University Malaysia campus. The gateway has been placed inside the Control Systems Laboratory located at the 3rd floor of the E0 building at the faculty of Engineering. The gateway is placed in front of a window which has been deliberately left open for better reception of data coming from both the sensor nodes.

Fig. 14 shows the range of areas which are covered by the LoRa network used in this study. The first sensor node placement was fixed under a bridge at a location 500 meters away from the gateway, while the initial location of the mobile second sensor node was 450 meters away from the gateway. Although LoRa is capable of transmitting data to long ranges, the presence of obstacles such as trees, terrain and buildings between the gateway and sensor nodes may affect the range of data transmission. It was observed that when the first and second sensor nodes were located 600 meters away from the gateway, the data packets sent began to drop. In

addition if the gateway was placed inside a building and away from windows the coverage of the LoRa network would have been further reduced. A spring antenna operating at a frequency of 433 Hz and a gain of 3dBi had been used in this study. Utilizing antennas with more superior characteristics may also increase the LoRa network coverage.

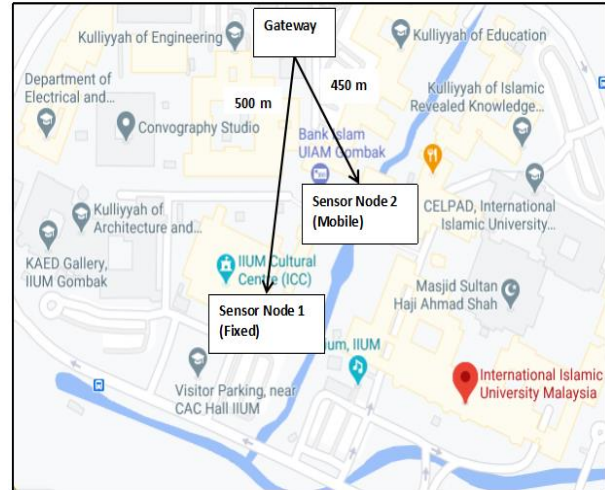


Fig. 14. Range for the coverage of the LoRa Network within the university campus

### VI. REAL TIME MONITORING USING FIXED AND MOBILE SENSOR NODES

Fig. 15 shows the internal view of the sensor node. The sensor node has a height of 8 cm, width of 5cm and length of 12 cm. This dimension is necessary to accommodate all the sensors, batteries, LoRa module and other electronic components within the weather-proof enclosure. A solar panel with a 6V and 3 Watt rating is placed on top of the sensor node. A smaller version of the sensor node can be achieved by designing a smaller printed circuit board with surface mount components instead of dual in line package components.

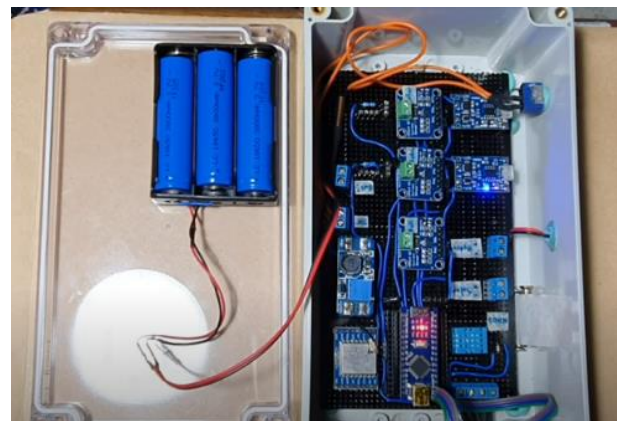


Fig. 15. Internal view of sensor node placed inside weather-proof container

Fig. 16 shows the fixed sensor node which contains a HC-SR04 ultrasonic sensor that is mounted underneath a bridge to monitor the water levels of the river. Fig. 17 shows the data collected from the fixed sensor node with

real time monitoring of increasing and decreasing water levels in the river for a period of 3 days in which heavy rain which had significantly raised river water levels had occurred twice as shown in the peaks of the graph. The water level is measured relative to the river base level. The initial variation in the river water level with respect to the river base level is between 1 to 1.3 meters. A total of 830 samples of data were transmitted to Losant each day. Initially the first 500 samples of data showed that the water levels were fluctuating only between 1 to 1.3 meters relative to the river base level which indicates that either no rain had occurred or only drizzling rain had occurred. The next 200 samples of water level readings reached beyond 1.3 meters relative to the river base level since during this period, heavy rain had occurred. The water levels had then returned to the 1 to 1.3 meters range relative to the river base after the rain had stopped and the water had subsided. A second incidence of rain had occurred the following day.



Fig. 16. Placement of sensor node underneath a bridge for river water level monitoring

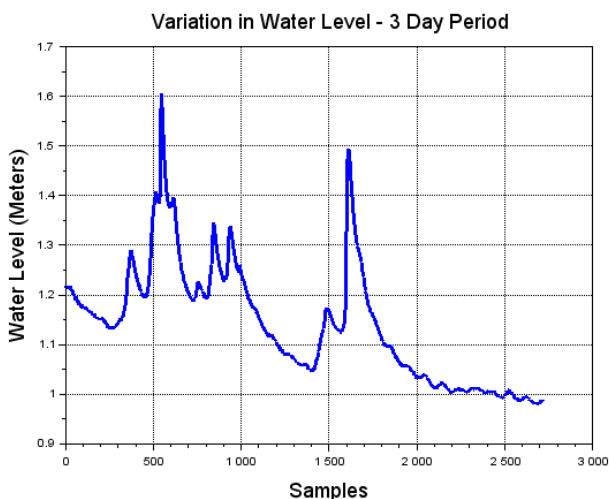


Fig. 17. Variation in river water levels - 3 day period

Monitoring the levels of Dissolved Oxygen in the river is particularly useful during and immediately after

flooding to determine if the river water has been contaminated by sewage, industrial and farming waste [17]. In addition Dissolved Oxygen measurements are one of the best indicators for the survival of aquatic life [18]–[23]. Fig. 18 shows the second sensor node which contains a Dissolved Oxygen sensor placed on a sensor buoy. The buoy can be moved around to float in different regions of the river and therefore functions as a mobile sensor node.



Fig. 18. Sensor buoy for dissolved oxygen measurements

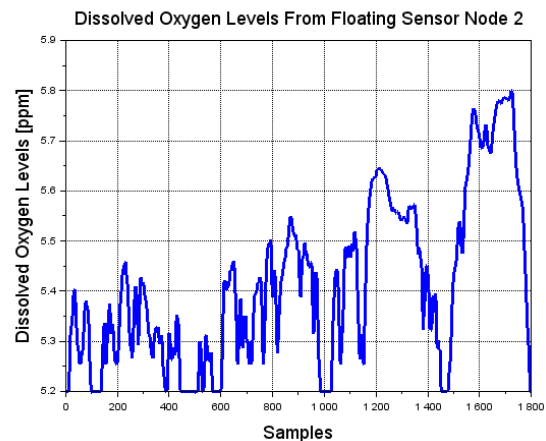


Fig. 19. Dissolved oxygen measurements from floating sensor buoy

Dissolved Oxygen levels are the highest during the morning and afternoon since photosynthesis depends on sunlight. On the contrary Dissolved Oxygen levels are the lowest at night due to the absence of sunlight and photosynthesis [24]. In natural freshwater systems such as rivers, lakes and streams, the depth of the water is also a contributing factor to the Dissolved Oxygen levels. Aquatic life require between 5-6 ppm of Dissolved Oxygen levels. Dissolved Oxygen levels below 3ppm are no longer suitable for aquatic life

Fig. 19 shows the Dissolved Oxygen levels measured using the mobile sensor node. The sensor node was placed on a buoy and allowed to float to different regions within the lake. The Dissolved Oxygen values range from 5.2 ppm to 5.8 ppm which indicates that the Dissolved Oxygen levels in this lake are suitable for aquatic life.

VII. CONCLUSION

In this study a method is proposed to preserve the battery life of the batteries used in the sensor nodes of a LoRa based WSN. This method consists of a combination of harvesting solar energy from the surroundings and also using a fuzzy logic algorithm for optimizing the frequency of data transmission to the cloud and hence reducing the number of charging and discharging cycles of the battery. Experiments were carried out to test the battery operation throughout a 30 day duration. The developed sensor nodes were deployed in a river to collect real time and reliable water level and dissolved oxygen data which is useful for flood monitoring.

CONFLICT OF INTEREST

The authors declare that there is no conflict of interest.

AUTHOR CONTRIBUTIONS

Mohd Aizat Mohd Yazid has conducted the literature review, conducted experiments and written the article. Ahmad Jazlan supervised the project and helped with writing the article. Mohd Zuhaili Mohd Rodzi was the field supervisor. Muhammad Afif Husman provided advice on hardware and software aspects. Abdul Rahman Afif designed and developed sensor nodes and programming for communication with gateway. All authors had approved the final version.

ACKNOWLEDGEMENT

The authors would like to thank the Malaysian Ministry of Higher Education for funding this research project under the Federal Research Grant Scheme - Grant No: FRGS19-057-0665 and FRGS16-053-0552.

APPENDIX A

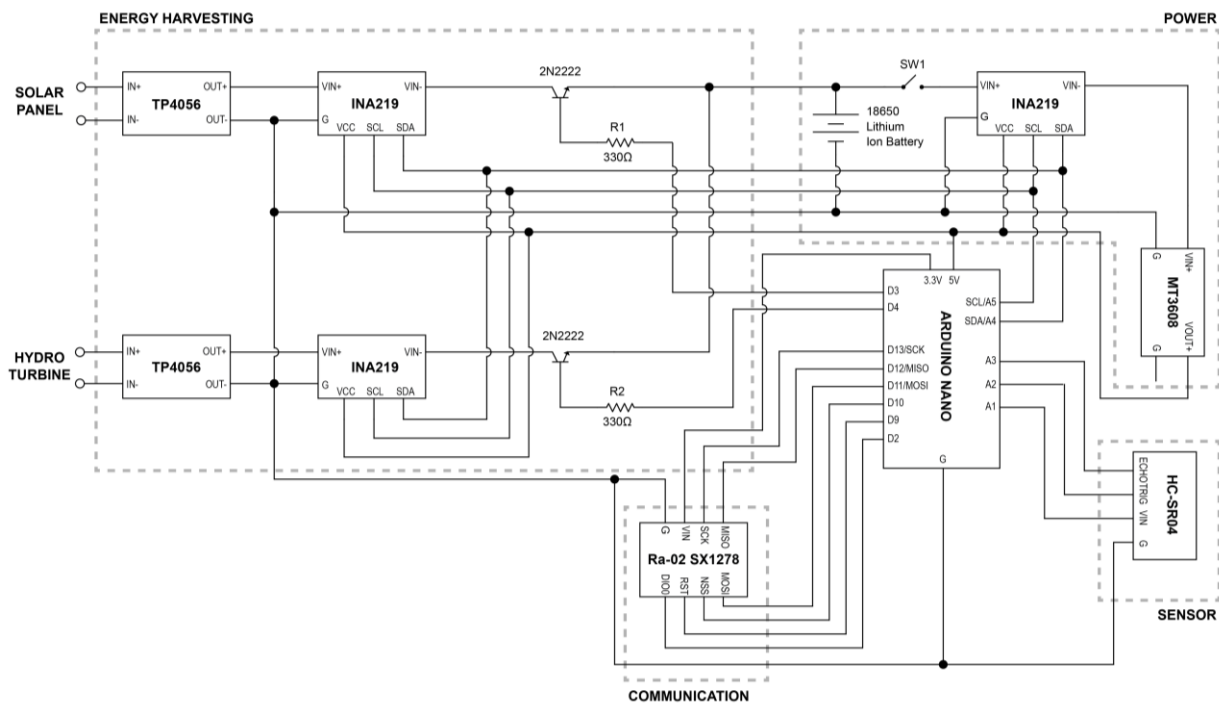


Fig. 20. Complete circuit schematic of the sensor nodes

REFERENCES

- [1] B. Burman, J. Kamruzzaman, G. Karmakar and S. Islam, "Low-Power wide-area networks: Design goals, architecture, suitability to use cases and research challenges," *IEEE Access*, vol. 8, pp. 17179-17220, 2020.
- [2] F. Wu, J. Redoute, and M. R. Yuce, "WE-Safe: A self-powered wearable IoT sensor network for safety applications based on LoRa," *IEEE Access*, vol. 6, pp. 40846-408530, 2020.
- [3] J. A. R. Azevedo and F. E. S. Santos, "Energy harvesting from wind and water for autonomous wireless sensor nodes," *IET Circuits, Devices and Systems*, vol. 6, no. 6, pp. 413-420, 2012.
- [4] B. Shi, V. Sreeram, D. Zhao, S. Duan, and J. Jiang, "A wireless sensor network-based monitoring system for freshwater fishpond aquaculture," *Biosystems Engineering*, vol. 172, no. 6, pp. 57-66, 2018.
- [5] C. Moreno, *et al.*, "RiverCore: IoT device for river water level monitoring over cellular communications," *Sensors*, vol. 19, no. 1, pp. 1-21, 2019.
- [6] M. T. Lazarescu, "Design of a WSN platform for long-term environmental monitoring for IoT applications," *IEEE Journal on Emerging and Selected Topics in Circuits and System*, vol. 3, no. 1, pp. 45-54, 2013
- [7] G. Mois, S. Folea, and T. Sanislav, "Analysis of three IoT-Based wireless sensors for environmental monitoring,"



*IEEE Transactions on Instrumentation and Measurement*, vol. 66, no. 8, pp. 2056-2064, 2017.

[8] S. D. T. Kelly, N. K. Suryadevara, and S. C. Mukhopadhyay, "Towards the implementation of IoT for environmental condition monitoring in homes," *IEEE Sensors Journal*, vol. 13, no. 10, pp. 3846-3853, 2013.

[9] Z. Tao, "Advanced wavelet sampling algorithm for IoT based environmental monitoring and management," *Computer Communications*, vol. 150, pp. 547-555, 2020.

[10] T. Ruan, Z. J. Chew, and M. Zhu, "Energy-Aware approaches for energy harvesting powered wireless sensor nodes," *Computer Communications*, vol. 17, no. 7 pp. 2165-2173, 2017.

[11] M. Mousa, X. Zhang, and C. Claude, "Flash flood detection in urban cities using ultrasonic and infrared sensors," *IEEE Sensors Journal*, vol. 16, no. 19 pp. 7204-7216, 2016.

[12] N. Kumar, A. Agrawal, and R. A. Khan, "Cost estimation of cellularly deployed IoT-enabled network for flood detection," *Iranian Journal of Computer Science*, vol. 2, pp. 53-64, 2019.

[13] B. Arshad, *et al.*, "Computer vision and IoT-Based Sensors in flood monitoring and mapping: A systematic review," *Sensors*, vol. 19, no. 22 pp. 53-64, 2019.

[14] M. Acosta-Coll, *et al.*, "Real-Time early warning system design for pluvial flash floods-a review," *Sensors*, vol. 18, no. 7, 2018.

[15] Q. Qian, B. Sun, X. Li, F. Sun, C. J. Lin, and L. Jiang, "Water quality evaluation on an urban stormwater retention pond using wireless sensor networks and hydrodynamic modeling," *Journal of Irrigation and Drainage Engineering*, vol. 145, no. 12, 2019.

[16] E. A. Basha, S. Ravela, and D. Rus, "Model-Based monitoring for early warning flood detection," in *Proc. 6th ACM Conference on Embedded Network Sensor Systems*, Association for Computing Machinery (ACM), New York, NY, USA, 2019, pp. 295-308.

[17] J. L. Steichen, *et al.*, "Microbial, physical, and chemical changes in galveston bay following an extreme flooding event, hurricane harvey," *Frontiers in Marine Science*, vol. 7, 2020.

[18] J. Huang, *et al.*, "Modelling dissolved oxygen depression in an urban river in China," *Water*, vol. 9, no. 7, 2107.

[19] A. T. Demetillo, M. V. Japitana, and E. B. Taboada, "A system for monitoring water quality in a large aquatic area using wireless sensor network technology," *Sustainable Environmental Research*, vol. 29, no. 12, 2019.

[20] I. Santin, *et al.*, "Dissolved oxygen control in biological wastewater treatments with non-ideal sensors and actuators," *Industrial & Engineering Chemistry Research*, vol. 58, no. 45, 2019.

[21] N. Zhu, *et al.*, "Prediction of dissolved oxygen concentration in aquatic systems based on transfer learning," *Computers and Electronics in Agriculture*, vol. 189, 2021.

[22] Y. Wei, *et al.*, "Review of dissolved oxygen detection technology: from laboratory analysis to online intelligent detection," *Sensors*, vol. 19, no. 18, 2019.

[23] H. Yu, *et al.*, "Dissolved oxygen content prediction in crab culture using a hybrid intelligent method," *Scientific Reports*, vol. 6, no. 27292, 2016.

[24] B. Keshtegar and S. Heddad, "Modeling daily dissolved oxygen concentration using modified response surface method and artificial neural network: A comparative study," *Neural Computing and Applications*, vol. 30, pp. 2995-3006, 2018.

Copyright © 2022 by the authors. This is an open access article distributed under the Creative Commons Attribution License ([CC BY-NC-ND 4.0](https://creativecommons.org/licenses/by-nc-nd/4.0/)), which permits use, distribution and reproduction in any medium, provided that the article is properly cited, the use is non-commercial and no modifications or adaptations are made.



**Mohd Aizat Mohd Yazid** is a Masters Student at the Department of Mechatronics Engineering, International Islamic University Malaysia. He is currently also an engineer at Elsa Energy Sdn Bhd. His research interests are Autonomous Ground Vehicles and UAV for Oil and Gas Platform Inspections



**Ahmad Jazlan** is an Assistant Professor at the Department of Mechatronics Engineering, International Islamic University Malaysia. His research interests are Control Theory, Model Order Reduction and Finite Element Analysis



**Mohd Zubaili Mohd Rodzi** is a Computer Science PhD student at Universiti Teknologi Malaysia. His Research Interests are in Industrial Automation, Ontology Networks and Internet of Things



**Muhammad Afif Husman** is an Assistant Professor at the Mechatronics Engineering Department, International Islamic University Malaysia. His research interests are in Biomedical Electronics, Instrumentation and Software Engineering.



**Abdul Rahman Afif** is a student at the Mechatronics Engineering Department, International Islamic University Malaysia. His research interests are Industrial Automation, Wireless Sensor Networks and Internet of Things.